Understanding graphene production by ionic surfactant exfoliation: A molecular dynamics simulation study

Peng Yang[1] and Feng Liu[2]
[1]*Department of Physics and Astronomy, University of Utah, Salt Lake City, Utah 84112, USA*
[2]*Department of Materials Science and Engineering, University of Utah, Salt Lake City, Utah 84112, USA*

(Received 9 May 2014; accepted 12 June 2014; published online 1 July 2014)

We have simulated sodium dodecyl sulfate (SDS) surfactant/water + bilayer graphene mixture system to investigate two mechanisms of graphene exfoliation: changing the interlayer distance and sliding away the relative distance. By calculating the total energy as a function of the interlayer (sliding-away) distance at different surface-coverage concentrations of SDS surfactant (SDS concentrations), we obtain the separation energy barriers underlying the two mechanisms and their dependence on SDS concentration. Overall, in the first process, the energy barrier can only be reduced by the SDS slightly, which is too big to be viable. While in the second process, the energy barrier can be first decreased continuously with the increasing SDS concentration until it almost completely disappear in the optimal SDS concentration range (1.5–2.0/nm^2) and then increase again with the further increase in SDS concentration. Therefore, the second sliding-away mechanism is a more viable separation process. The analysis of SDS anion density profile on the graphene surface indicates that the graphene-surfactant interaction plays an important role in the separation process by stabilizing the separated graphene sheet. © *2014 AIP Publishing LLC*.
[http://dx.doi.org/10.1063/1.4885159]

I. INTRODUCTION

Graphene is a two-dimensional, one atom thick honeycomb lattice made of *sp*-bonded carbon atoms,[1,2] which is also the basic building block of graphite, carbon nanotubes, fullerenes, and so on. Because of its extraordinary electronic, mechanical, and optical properties, it has attracted a wide range of research attention.[3–6] Although fundamental research is still carried out on graphene,[7,8] more and more attention is being paid to its potential applications, such as transistors,[9] electrode,[10] solar cells,[11] supercapacitors,[12] and biodevices.[13] To realize its potential applications, however, mass production of high quality graphene must be achieved.

The high quality yet small-piece graphene produced by using micro-mechanically cleavage method has been used in fundamental investigation of its properties, but it is not suitable for large-scale, easy, and cheap mass production.[14] The development of large-scale, high-quality graphene growth method has drawn a lot of attention and progressed rapidly in the past decade. Segregation of carbon from carbon-saturated metals (Ni/Fe),[15] chemical vapor deposition (CVD) on metal substrates,[16] epitaxial growth on silicon carbide,[17] graphite oxide reduction,[18] has been explored with certain success, but they either suffer from the difficulty of integrating the sample into devices[14] or disrupting the intrinsic electronic structure of graphene.[18]

Recently, an alternative top-down liquid exfoliation approach to produce cheap, large-scale graphene has been proposed,[19] which has also been extended to separating other layered materials.[20,21] In these solution-phase techniques, raw material, such as graphite powder, was first prepared and then dispersed in organic solvents or aqueous surfactant solutions. Shock wave was generated by sonication which breaks apart the graphite flakes. After removing the aggregates by centrifugation, a homogeneous liquid dispersion, including separated monolayer and few-layer graphene, was obtained. The separated graphene has been stabilized by the attachment of solvent molecules on the surface of graphene. A key point of this method is that the surface energy of solvent molecules has to match that of graphite, which can make the separated graphene stable.[22]

Based on the experience of dispersions of carbon nanotubes, Coleman's group has shown that N-methylpyrrolidone (NMP) and N, N-dimethylacetamide (DMA) are efficient at dispersing graphene,[23] and improved their dispersion by using cheap, low-boiling, safe, and user-friendly surfactants/water mixture solution.[24] Bourlinos and Stubos have found some perfluorinated aromatic molecules, such as hexafluorobenzene (C_6F_6) and octafluorotoluene ($C_6F_5CF_3$) which can also be used to prepare solubilized graphenes.[25] Some other liquid exfoliation studies have also been reported by using a wide range of solvents.[26–31]

By using surface energy and Hansen solubility parameter data analysis, Coleman and co-workers have shown that solvent-graphene surface matching is the dominating factor in the dispersion process.[22] This semiempirical approach can provide us with some useful information in discovering new solvents; however, it does not give a complete, clear picture of understanding the dispersion process. On the other hand, molecular dynamics (MD) simulations have been widely used to study the complicated liquid systems for a long time. Important solvents, such as water, surfactant, ionic liquids, and their mixture systems with carbon nanotube (or graphite) have been studied. Especially, Blankschtein and co-workers have studied graphene/polar solvents systems and explained the stabilization of the graphene sheets by calculating

potential of mean force and kinetic theory analysis.[32] Later, they also studied ionic surfactant sodium cholate (SC) on a monolayer graphene sheet and calculated electrostatic potential around graphene-SC assembly.[33] Most recently, Yang and Fu have studied the interfacial mechanics for different solvents and concluded that the confined solvent molecules between graphene sheets contribute significantly to exfoliation and stabilization process.[34]

However, sodium dodecyl sulfate (SDS) as an important ionic surfactant, which is composed of positively charged sodium ions and anions with a long non-polar carbon tail, plays an important role in separating carbon nanotubes as well as an effective solvent in separating graphite has not been studied systematically. In order to better understand the liquid dispersion of graphene, SDS/water + graphene mixture system need to be investigated. The separation mechanism, the role of SDS concentration, and corresponding surface morphology are all interesting questions remain to be answered.

In this paper, we have carried out MD simulations of SDS/water + bilayer graphene mixture system at a variety of surface-coverage concentrations of SDS surfactant (SDS concentrations). By calculating the total energy as a function of interlayer (sliding-away) distance, we obtain the energy barrier and surface morphology at different SDS concentrations. Then we studied surfactant distribution along separation path (interlayer or sliding-away distance). We compared these two separation mechanisms and analyzed the role of SDS concentration in each process.

II. SIMULATION METHODOLOGY

In this work, the classical all-atom MD simulations were done by GROMACS package.[35] The total potential energy is given by the expression

$$V = \sum_{bonds} k_b(r - r_{eq}) + \sum_{angles} k_\theta(\theta - \theta_{eq}) + \sum_{dihedrals} \frac{v_n}{2}(1 + \cos(n\varnothing - \gamma)) + \sum_i \sum_{j>i} \left(\frac{a_{ij}}{r_{ij}^{12}} - \frac{b_{ij}}{r_{ij}^{6}} + \frac{q_{ij}}{r_{ij}} \right). \quad (1)$$

In the above equation, the force field parameters for SDS are provided from the standard Amber force field. As for the model of graphene, we choose a rigid-body model which only considers the Van der Waals (VdW) interaction between different graphene layers[36] and takes parameters suggested in the literature.[37] This model ignores the intramolecular interactions within graphene, and hence atomic vibration and small bond distortion during graphene exfoliation process. This should be a good approximation because these effects will not significantly influence the separation energy barrier, which is dominated by the intermolecular interactions, i.e., the graphene-graphene and graphene-surfactant interaction. The water model is TIP3P[38] which is compatible with Amber force Field. The partial charges for the anion of SDS were calculated by fitting *ab initio* electrostatic potentials with RESP package,[39] while the charge of sodium ion and carbon atoms in graphene is +1, 0, respectively. The *ab initio* calculation was done with Gaussian 03 package.[40]

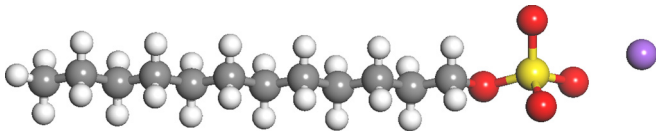

FIG. 1. The structure of SDS molecule. The gray, white, red, yellow, and purple balls represent carbon, hydrogen, oxygen, sulfur, and sodium atoms, respectively.

The system studied in this work consists of SDS surfactant/water + bilayer graphene mixture. The structure of SDS is shown in Fig. 1. The ion pairs in surfactant, number of atoms in bilayer graphene, and number of water molecules in different SDS concentration are given in Table I. The initial simulation configuration was randomly generated by Gromacs package followed by a quick relaxation, then the relaxed configuration was simulated with a constant number of particle, pressure and temperature (NPT) simulation for 8 ns at room temperature (T = 298.15 K) and the total energy of the last 3 ns was calculated. To make sure the system reaches the equilibrium, annealing process was then used: the final configuration obtained from the NPT simulation was again equilibrated at T = 1000 K in a constant number of particle, volume and temperature (NVT) simulation and the temperature was gradually lowered to 800 K, 600 K, 400 K, and room temperature. We repeat the annealing process for two or three times. Finally, the production run of NVT simulation at room temperature was carried out for 3 ns. All the data are taken from this period.

The timestep used in the simulations is 1 fs, while the cutoff of 12 Å for VdW interaction is used. Long-range electrostatic interactions were treated using the particle mesh Ewald (PME) summation method.[41,42] Berendsen coupling is used for maintaining a pressure of 1 atm in NPT simulations and velocity rescales were used in all the simulations.[43]

III. RESULTS AND DISCUSSIONS

A. Graphene exfoliation by variation of interlayer distance (Fig. 2(a))

To simulate the exfoliation process, we consider the variation of the interlayer distance of bilayer graphene at six different SDS concentrations by calculating the total energy as a function of interlayer distance (Fig. 3). The two large, parallel single-layer graphene sheets have been put in a big box form an AA-stacked bilayer graphene. The interlayer

TABLE I. Size of the SDS surfactant/water + bilayer graphene simulation system.

SDS concentration (/nm^2)	Number of carbon atoms (graphite)	Number of ion pairs (SDS)	Number of water molecules
0	2800	0	9281
0.5	2800	70	9281
1.0	2800	140	9281
1.5	2800	216	9281
2.0	2800	280	9281
2.8	2800	393	9281

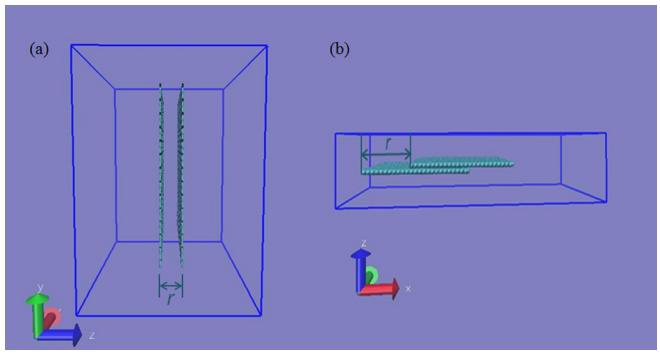

FIG. 2. (a) Schematic graph of variation of interlayer distance of two parallel single-layer graphene sheets; (b) schematic graph of variation sliding away distance of two single-layer graphene sheets. Blue is the simulation box and green is graphene.

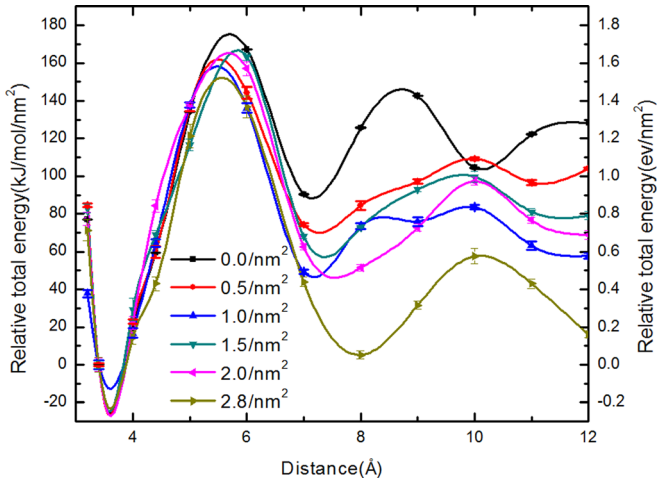

FIG. 3. Relative total energy (potential energy profile) of SDS surfactant/water + bilayer graphene mixtures at different SDS concentrations as a function of interlayer distance.

distance r varies from about 3 Å to 12 Å. By extracting the data from the production run, the relative total energy (potential energy) profile is shown in Fig. 3 (we take the energy at $r = 3.4$ Å as our reference of zero energy). In addition, the average numbers of SDS anions confined in between the graphene sheets are also calculated and shown in Fig. 4.

From Fig. 3, we found that the minimum energies in the mixture systems are all located at the distance r around 3.6 Å, which is slightly larger than the equilibrium layer-layer distance of pure graphite (3.35 Å). This can be understood by the attractive interaction between graphene and solvent. There are three major (solvent-solvent, solvent-graphene, and graphene-graphene) interactions in the mixture system compared with one (graphene-graphene) interaction in pure bilayer graphene system, the competition between graphene-graphene and solvent-graphene interaction changes the equilibrium separation distance which varies slightly with SDS concentration as shown in Fig. 3. The energy increases quickly for 3.4 Å $< r <$ 6 Å, indicating that the graphene-graphene VdW interaction still dominates in the mixture system. With the increasing distance r, the energy oscillates for 6 Å $< r <$ 12 Å and the systems finally reach the complete separation of the bilayer graphene at $r = 12$ Å. From 6 Å to 12 Å, two more local minima form which means the solvent-graphene interaction begins to dominate and gradually overcomes the graphene-graphene interaction. From Figs. 3 and 4(a), we discover a corresponding relationship between the confined number of SDS anions in between two graphene sheets and the potential energy profile. For $r < 7$ Å, because of a too small space, no SDS anions can be confined. Then there is a quick increase in confined number of SDS anions and they form one layer of SDS (7 Å $<= r <=$ 9 Å), which contributes to the first local minimum in Fig. 3. Then we have a short range for almost no change of the number of confined SDS anions (still one layer SDS) for 9 Å $\leq r <$ 11 Å, which contributes to the local maximum at $r \approx 10$ Å. For $r \geq 11$ Å, the number of SDS anions increases again and two layers of SDS form. Here, we need to point out the black line in Fig. 3, which shows the potential energy profile along the separation distance in water + bilayer graphene system (no SDS). Similar to SDS surfactant/water + bilayer graphene system, the confinement of water molecules in between two graphene sheets contributes to two local minima

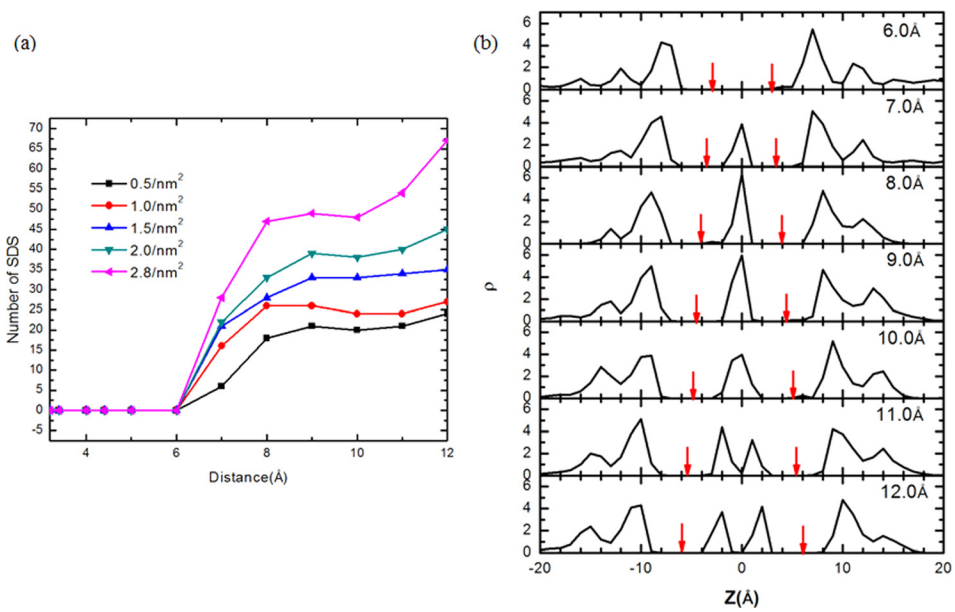

FIG. 4. SDS anion distribution analysis in SDS surfactant/water + bilayer graphene mixture system. (a) Number of SDS anions confined in inner space between two parallel single-layer graphene sheets. (b) Normalized density profile of SDS anions as a function of interlayer distance at SDS concentration = 2.0/nm^2 (The red arrows give the locations of two graphene sheets).

at $r \approx 7$, 10 Å. This suggests that water has a weak interaction with graphene. However, even at very large separation distances, the energy of water + bilayer graphene system is still high, which means the separated graphene state is not as stable as in SDS surfactant/water solution. Therefore, water alone cannot effectively lower the separation energy barrier of bilayer graphene because of weaker surface affinity of water on graphene surface. The following discussion will be focused on the role of SDS concentrations.

To see the transitions clearly, we plot SDS anion density profile along z axis (interlayer distance) and extract snapshots at different SDS concentrations. Because of the similarity at all concentrations, here we only show the plots at SDS concentration = 2.0/nm^2 (Fig. 4(b)). Since there is no SDS anions confined inside the interlayer graphene inner space at small distances, the plot begins with distance $r > 6$ Å. When 7 Å $\leq r \leq$ 10 Å, there is one peak inside the interlayer graphene inner space in Fig. 4(b). Because the graphene-graphene VdW interaction disappears quickly after moving further away from the graphite equilibrium distance, SDS anions have been attracted into the open space and total energy attains a local minimum here at around $7 \sim 8$ Å. In this region, we found the number of SDS anions first increases, then stabilizes (almost no change or slight decrease). This is consistent with Fig. 3, because after the local minimum at r around 7 Å, the energy increases and reaches a local maximum at r around 10 Å. Further increasing the distance from the local maximum, the number of SDS anions increases again and forms two layers, and correspondingly the energy decreases again. The zero layer, one layer, and two layers of SDS in between the two graphene sheets are also shown in snapshots of Fig. 5. It can be understood as the attractive interaction between SDS anions and graphene drives more and more SDS anions to move into the inner space between two graphene sheets when interlayer distance increases. The number of SDS anions increases gradually to form one layer and two layers of SDS until completely separating the graphene sheets.

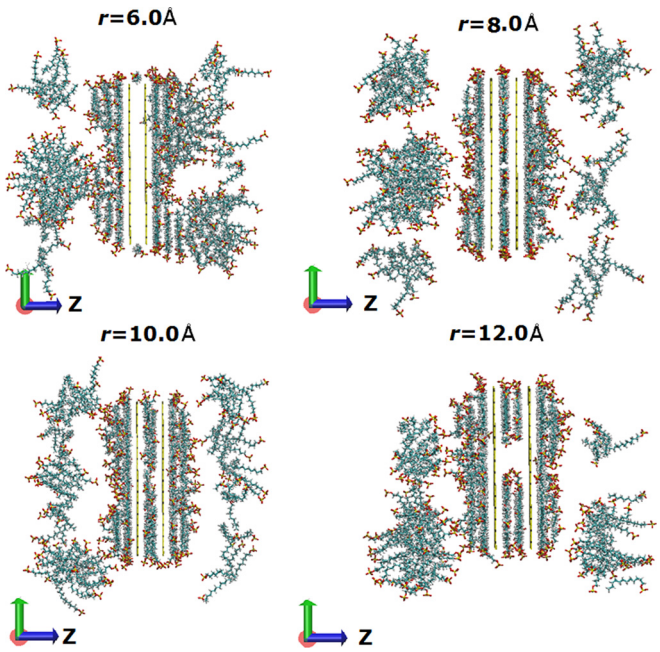

FIG. 5. Snapshots from production run at four different interlayer distances (SDS concentration = 2.0/nm^2, we only show SDS anions and graphene sheet to make it clear). Red represents oxygen in SDS, yellow represents graphene, and cyan represents tail of SDS anion.

From the potential energy profile (Fig. 3), we can define local energy barriers of the separation process at different SDS concentrations, and the calculated results are shown in Table II. From Table II, we can see that compared with water + bilayer graphene system without SDS which has a first and second barrier (2.0 eV/nm^2 and 0.6 eV/nm^2), both the first and second energy barrier are smaller in the SDS surfactant/water + bilayer graphene mixture system at different SDS concentrations which means SDS surfactant/water + bilayer graphene system is better than water + bilayer graphene system in separating graphene. However, the decrease in energy barrier by SDS via this direct separation process is insignificant by ~0.1–0.3 eV. This indicates that direct changing interlayer distance is unlikely the most viable mechanism of separation. Therefore, below we investigate a different mechanism.

B. Graphene exfoliation by sliding away the relative distance of graphene (Fig. 2(b))

In the above considered mechanism of bilayer graphene exfoliation by changing the interlayer distance, strong VdW interaction between graphene sheets must be overcome. Because the separation path is parallel to the VdW interaction direction, it is energy consuming compared with another possible exfoliation path: sliding away the relative distance of graphene (Fig. 2(b)). Here again, we calculate the total energy as a function of sliding-away distance at different SDS concentrations; the distance varies from about 3.4 Å to 7.0 nm (complete separation). The calculated results are shown in Fig. 6 (the energy at $r = 3.4$ Å as the reference of zero energy). As we can see, when the SDS concentration is smaller or equal to 1.0/nm^2, the energy generally goes up with the increasing sliding-away distance. The energy oscillates at SDS concentration = 1.5 (or 2.0)/nm^2 when the sliding-away distance increases, with no obvious trend. The energy curve at SDS concentrations of 2.8/nm^2 shows a strong oscillation compared with that at SDS concentrations of 1.5 (or 2.0)/nm^2, and seems to increase slowly with the increasing sliding-away distance, similar to those at SDS concentrations $\leq$1.0/nm^2. Then we use a linear function to fit these energy curves, the slope of each fit can tell us the increasing rate of the energy curve. When slope > 0, the energy still increases as the

TABLE II. Energy barriers in variation of interlayer distance mechanism.

SDS concentration (/nm^2)	First energy barrier (eV/nm^2)	Second energy barrier (eV/nm^2)
0.0	2.0	0.6
0.5	1.9	0.4
1.0	1.7	0.4
1.5	1.9	0.4
2.0	1.9	0.5
2.8	1.7	0.5

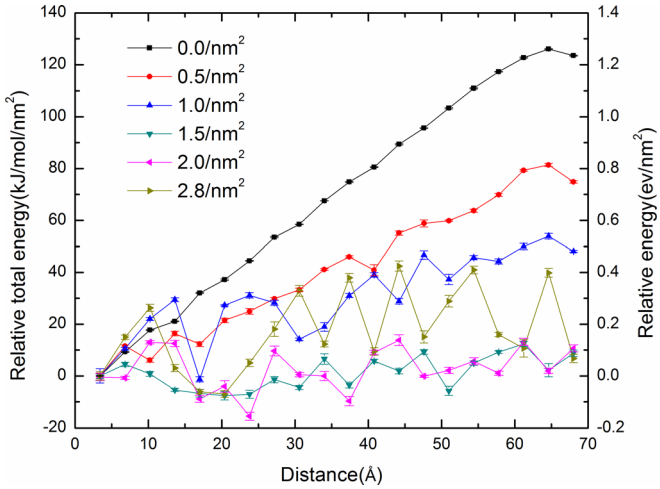

FIG. 6. Relative total energy (potential energy) profile of SDS surfactant/water + bilayer graphene mixtures at different SDS concentrations as a function of sliding-away distance.

sliding-away distance increases, and larger slope means a harder separation process. For slope ≈ 0, the energy curve basically does not go up with the increasing sliding-away distance, which means an easier separation process. Our fit slopes for six different SDS concentrations are 2.06, 1.24, 0.54, 0.22, −0.02, and 0.31, respectively. Then we calculated the energy barrier in this process (the energy difference between the maximum state and the initial state). From the calculated results shown in Table III, we found that the energy barrier decreases as the SDS concentration increases, from 0.5/nm^2 to SDS concentration of 1.5/nm^2, at which there is a minimum barrier of 0.12 eV/nm^2, then it increases to 0.4 eV/nm^2 at SDS concentration = 2.8/nm^2.

Therefore, for best bilayer graphene separation, SDS concentration is around 1.5–2.0/nm^2. This can be understood as follows: when there is no surfactant, the dominant interaction is graphene-graphene VdW interaction, which decreases

TABLE III. Energy barriers in variation of sliding-away distance mechanism.

SDS concentration (/nm^2)	Energy barrier (eV/nm^2)
0.0	1.26
0.5	0.81
1.0	0.54
1.5	0.12
2.0	0.13
2.8	0.4

quickly with the increasing sliding-away distance. When adding surfactants into the system, increasing sliding-away distance means more surface area of graphene is exposed to solvents, and more surfactants are attracted to the exposed surface, which lower the energy compared with water + bilayer graphene system. At low SDS concentrations (≤1.0/nm^2), the graphene-surfactant interaction is not strong enough to compensate the total loss of the graphene-graphene VdW interaction when sliding away graphene sheet, the energy increases. While at higher SDS concentrations (≤2.0/nm^2), the graphene-surfactant interaction is becoming so strong and sufficiently compensates the energy lost of the graphene-graphene VdW interaction, which makes no obvious change of the energy. At maximum SDS concentration (=2.8/nm^2), the graphene-surfactant interaction becomes weaker again, so the energy goes up again. Other interactions perturb the energy and make the energy curve oscillates. From the analysis above, we conclude that at the critical SDS concentrations (1.5–2.0/nm^2, when slope ≈ 0), the energy barrier almost disappears, which is the best for graphene separation.

Apparently, the graphene-surfactant interaction plays an important role in decreasing the separation energy barrier. We plot the SDS anion density profile along the separation path (x axis) and snapshots at SDS concentration = 2.0/nm^2 (Figs. 7 and 8). Before the separation, the SDS self-

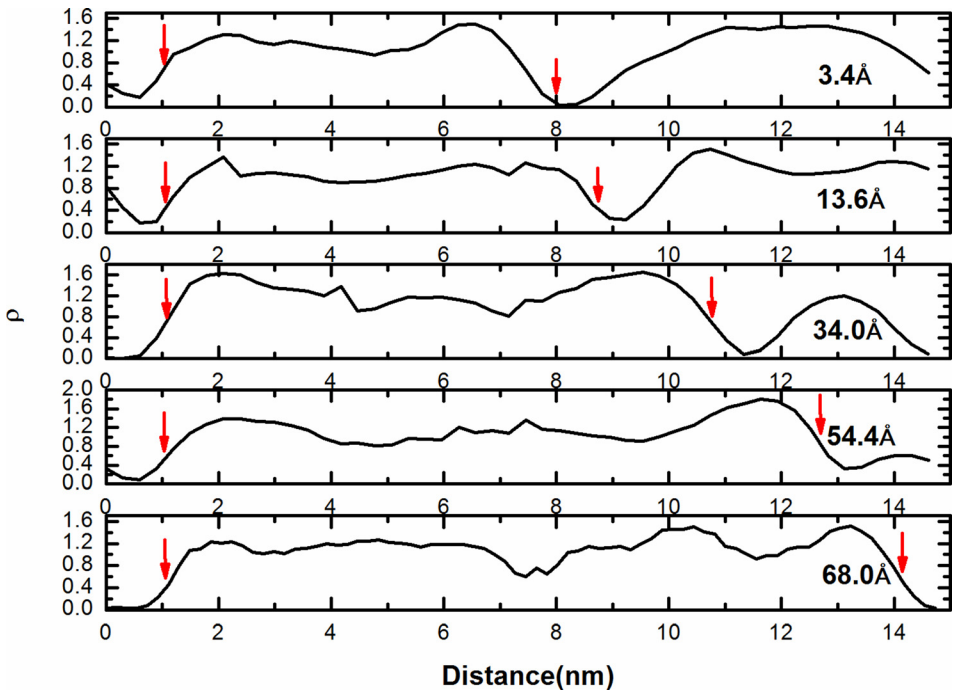

FIG. 7. Normalized density profile of SDS as a function of sliding-away distance at SDS concentration = 2.0/nm^2 (The red arrows give the locations of two graphene sheets edges).

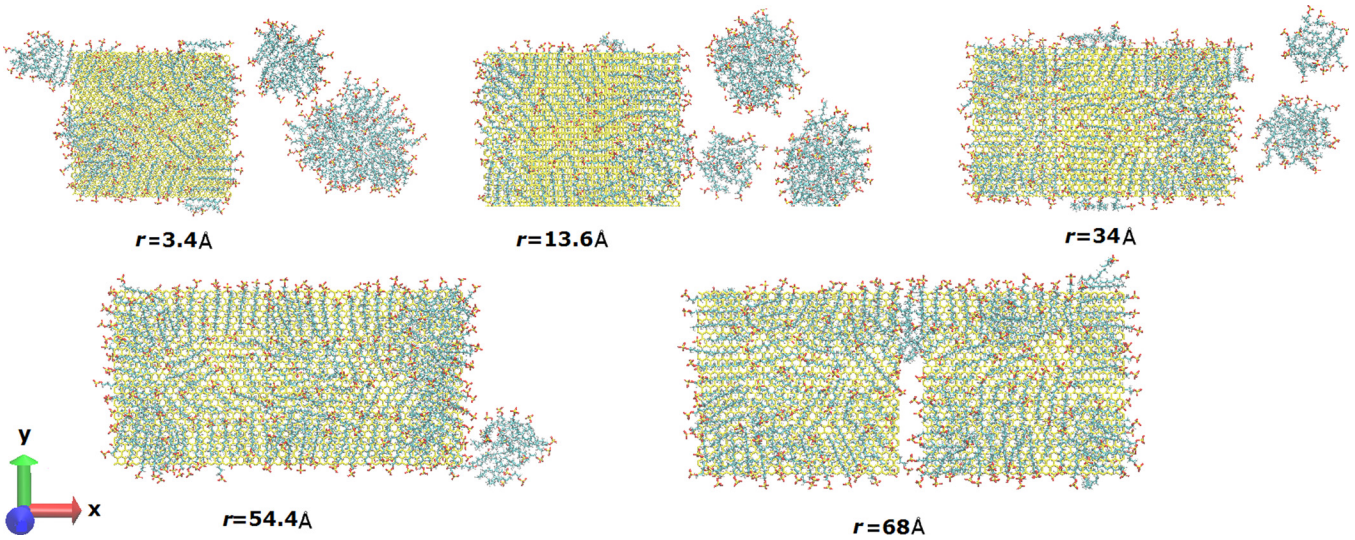

FIG. 8. Snapshots from production run at five different sliding away distances (SDS concentration = 2.0/nm^2, only SDS anions and graphene sheet are shown to make it clear). Red represents oxygen in SDS, yellow represents graphene, and cyan represents tail of SDS anion.

assembles to form big micelles (Fig. 8), which lowers the energy and makes the system a stable state. When we increase the sliding-away distance, the attractive graphene-surfactant interaction forces SDS to move to the exposed surface of graphene which compensates the loss of graphene-graphene interaction. So the micelle structure has been destroyed gradually and the entire graphene surface has been covered with SDS. The attachment of SDS on graphene surface gives the maximum graphene-surfactant interaction and stabilizes the separated graphene sheets.

IV. CONCLUSIONS

In this work, we have studied two separation mechanisms of SDS surfactant/water + bilayer graphene mixture systems at various SDS concentrations: one is by changing the interlayer distance between graphene sheets and another one is by sliding away the relative distance between graphene sheets. By changing the interlayer distance (the separation is along the graphene-graphene VdW direction), the graphene-graphene VdW interaction is replaced by graphene-solvent interaction gradually. Because the surfactant-graphene VdW interaction is stronger than the water-graphene interaction, energy barrier in SDS/water + bilayer graphene system can be decreased by ~0.1–0.3 eV compared with water + bilayer graphene system, but it is still not a viable separation process because of high energy barrier (1.7 eV/nm^2). When changing the relative distance (the separation path is perpendicular to VdW direction), energy barrier can be lowed quickly to a very small value (0.12 eV/nm^2) at certain surfactant concentrations (1.5–2.0/nm^2) which is good for exfoliation. Our results show that the sliding-away mechanism is more likely to be responsible for liquid exfoliation process because the surfactant-graphene interaction is maximized which is critical to the separation process.

ACKNOWLEDGMENTS

This work is supported by DOE-BES (Grant No. DEFG02-04ER46148). We thank for The Center for High Performance Computing at University of Utah for doing the parallel computer simulations. We also thank Dr. Hepeng Ding and Dr. Miao Liu for their helpful discussions.

[1]K. S. Novoselov, A. K. Geim, S. Morozov, D. Jiang, Y. Zhang, S. Dubonos, I. Grigorieva, and A. Firsov, Science **306**(5696), 666–669 (2004).
[2]K. S. Novoselov, D. Jiang, F. Schedin, T. J. Booth, V. V. Khotkevich, S. V. Morozov, and A. K. Geim, Proc. Natl. Acad. Sci. U.S.A. **102**(30), 10451–10453 (2005).
[3]A. K. Geim and K. S. Novoselov, Nature Mater. **6**(3), 183–191 (2007).
[4]C. Lee, X. Wei, J. W. Kysar, and J. Hone, Science **321**(5887), 385–388 (2008).
[5]A. K. Geim, Science **324**(5934), 1530–1534 (2009).
[6]K. S. Novoselov, V. Fal, L. Colombo, P. Gellert, M. Schwab, and K. Kim, Nature **490**(7419), 192–200 (2012).
[7]A. C. Neto, F. Guinea, N. Peres, K. S. Novoselov, and A. K. Geim, Rev. Mod. Phys. **81**(1), 109 (2009).
[8]S. D. Sarma, S. Adam, E. Hwang, and E. Rossi, Rev. Mod. Phys. **83**(2), 407 (2011).
[9]Q. Yan, B. Huang, J. Yu, F. Zheng, J. Zang, J. Wu, B.-L. Gu, F. Liu, and W. Duan, Nano Lett. **7**(6), 1469–1473 (2007).
[10]K. S. Kim, Y. Zhao, H. Jang, S. Y. Lee, J. M. Kim, K. S. Kim, J.-H. Ahn, P. Kim, J.-Y. Choi, and B. H. Hong, Nature **457**(7230), 706–710 (2009).
[11]Y. Zhang, C. Hui, R. Sun, K. Li, K. He, X. Ma, and F. Liu, Nanotechnology **25**(13), 135301 (2014).
[12]Y. Zhu, S. Murali, M. D. Stoller, K. Ganesh, W. Cai, P. J. Ferreira, A. Pirkle, R. M. Wallace, K. A. Cychosz, and M. Thommes, Science **332**(6037), 1537–1541 (2011).
[13]R. Nair, P. Blake, J. Blake, R. Zan, S. Anissimova, U. Bangert, A. Golovanov, S. Morozov, A. Geim, and K. Novoselov, Appl. Phys. Lett. **97**(15), 153102 (2010).
[14]P. Avouris and C. Dimitrakopoulos, Mater. Today **15**(3), 86–97 (2012).
[15]Q. Yu, J. Lian, S. Siriponglert, H. Li, Y. P. Chen, and S.-S. Pei, Appl. Phys. Lett. **93**(11), 113103 (2008).
[16]A. Obraztsov, E. Obraztsova, A. Tyurnina, and A. Zolotukhin, Carbon **45**(10), 2017–2021 (2007).
[17]A. Charrier, A. Coati, T. Argunova, F. Thibaudau, Y. Garreau, R. Pinchaux, I. Forbeaux, J.-M. Debever, M. Sauvage-Simkin, and J.-M. Themlin, J. Appl. Phys. **92**(5), 2479–2484 (2002).
[18]S. Stankovich, D. A. Dikin, R. D. Piner, K. A. Kohlhaas, A. Kleinhammes, Y. Jia, Y. Wu, S. T. Nguyen, and R. S. Ruoff, Carbon **45**(7), 1558–1565 (2007).
[19]A. A. Green and M. C. Hersam, J. Phys. Chem. Lett. **1**(2), 544–549 (2010).
[20]J. N. Coleman, M. Lotya, A. O'Neill, S. D. Bergin, P. J. King, U. Khan, K. Young, A. Gaucher, S. De, and R. J. Smith, Science **331**(6017), 568–571 (2011).
[21]V. Nicolosi, M. Chhowalla, M. G. Kanatzidis, M. S. Strano, and J. N. Coleman, Science **340**(6139), 1226419 (2013).

[22]J. N. Coleman, Acc. Chem. Res. **46**(1), 14–22 (2013).
[23]Y. Hernandez, V. Nicolosi, M. Lotya, F. M. Blighe, Z. Sun, S. De, I. McGovern, B. Holland, M. Byrne, and Y. K. Gun'Ko, Nat. Nanotechnol. **3**(9), 563–568 (2008).
[24]M. Lotya, Y. Hernandez, P. J. King, R. J. Smith, V. Nicolosi, L. S. Karlsson, F. M. Blighe, S. De, Z. Wang, and I. McGovern, J. Am. Chem. Soc. **131**(10), 3611–3620 (2009).
[25]A. B. Bourlinos, V. Georgakilas, R. Zboril, T. A. Steriotis, and A. K. Stubos, Small **5**(16), 1841–1845 (2009).
[26]J. Lu, J.-X. Yang, J. Wang, A. Lim, S. Wang, and K. P. Loh, ACS Nano **3**(8), 2367–2375 (2009).
[27]X. Wang, P. F. Fulvio, G. A. Baker, G. M. Veith, R. R. Unocic, S. M. Mahurin, M. Chi, and S. Dai, Chem. Commun. **46**(25), 4487–4489 (2010).
[28]R. J. Smith, M. Lotya, and J. N. Coleman, New J. Phys. **12**(12), 125008 (2010).
[29]X. Zhang, A. C. Coleman, N. Katsonis, W. R. Browne, B. J. van Wees, and B. L. Feringa, Chem. Commun. **46**(40), 7539–7541 (2010).
[30]D. Nuvoli, L. Valentini, V. Alzari, S. Scognamillo, S. B. Bon, M. Piccinini, J. Illescasd, and A. Mariani, J. Mater. Chem. **21**, 3428–3431 (2011).
[31]J. Zhao, Z. Wang, Q. Zhao, and B. Xing, Environ. Sci. Technol. **48**(1), 331–339 (2014).
[32]C.-J. Shih, S. Lin, M. S. Strano, and D. Blankschtein, J. Am. Chem. Soc. **132**(41), 14638–14648 (2010).
[33]S. Lin, C.-J. Shih, M. S. Strano, and D. Blankschtein, J. Am. Chem. Soc. **133**(32), 12810–12823 (2011).
[34]C. Fu and X. Yang, Carbon **55**, 350–360 (2013).
[35]E. Apol, R. Apostolov, H. Berendsen, A. Van Buuren, P. Bjelkmar, R. Van Drunen, A. Feenstra, G. Groenhof, P. Kasson, and P. Larsson, *Groamcs User Manual 4.5.4* (Royal Institute of Technology and Uppsala University, Stockholm and Uppsala, Sweden, 2010).
[36]D. Yu and F. Liu, Nano Lett. **7**(10), 3046–3050 (2007).
[37]L. Battezzati, C. Pisani, and F. Ricca, J. Chem. Soc., Faraday Trans. 2 **71**, 1629–1639 (1975).
[38]W. L. Jorgensen, J. Chandrasekhar, J. D. Madura, R. W. Impey, and M. L. Klein, J. Chem. Phys. **79**(2), 926–935 (1983).
[39]C. I. Bayly, P. Cieplak, W. Cornell, and P. A. Kollman, J. Phys. Chem. **97**(40), 10269–10280 (1993).
[40]M. J. Frisch, G. W. Trucks, H. B. Schlegel, G. E. Scuseria, M. A. Robb, J. R. Cheeseman, J. A. Montgomery, Jr., T. Vreven, K. N. Kudin, J. C. Burant, J. M. Millam, S. S. Iyengar, J. Tomasi, V. Barone, B. Mennucci, M. Cossi, G. Scalmani, N. Rega, G. A. Petersson, H. Nakatsuji, M. Hada, M. Ehara, K. Toyota, R. Fukuda, J. Hasegawa, M. Ishida, T. Nakajima, Y. Honda, O. Kitao, H. Nakai, M. Klene, X. Li, J. E. Knox, H. P. Hratchian, J. B. Cross, V. Bakken, C. Adamo, J. Jaramillo, R. Gomperts, R. E. Stratmann, O. Yazyev, A. J. Austin, R. Cammi, C. Pomelli, J. W. Ochterski, P. Y. Ayala, K. Morokuma, G. A. Voth, P. Salvador, J. J. Dannenberg, V. G. Zakrzewski, S. Dapprich, A. D. Daniels, M. C. Strain, O. Farkas, D. K. Malick, A. D. Rabuck, K. Raghavachari, J. B. Foresman, J. V. Ortiz, Q. Cui, A. G. Baboul, S. Clifford, J. Cioslowski, B. B. Stefanov, G. Liu, A. Liashenko, P. Piskorz, I. Komaromi, R. L. Martin, D. J. Fox, T. Keith, M. A. Al-Laham, C. Y. Peng, A. Nanayakkara, M. Challacombe, P. M. W. Gill, B. Johnson, W. Chen, M. W. Wong, C. Gonzalez, and J. A. Pople, GAUSSIAN 03, Revision C.02, Gaussian, Inc., Wallingford, CT, 2004.
[41]T. Darden, D. York, and L. Pedersen, J. Chem. Phys. **98**(12), 10089–10092 (1993).
[42]U. Essmann, L. Perera, M. L. Berkowitz, T. Darden, H. Lee, and L. G. Pedersen, J. Chem. Phys. **103**(19), 8577–8593 (1995).
[43]H. J. Berendsen, J. P. M. Postma, W. F. van Gunsteren, A. DiNola, and J. Haak, J. Chem. Phys. **81**(8), 3684–3690 (1984).